Catalysis Today 164 (2011) 74–79

Contents lists available at ScienceDirect

Catalysis Today

journal homepage: www.elsevier.com/locate/cattod

Enhanced performance of Ru nanoparticles confined in carbon nanotubes for CO preferential oxidation in a H_2-rich stream

Bodong Li, Chao Wang, Guangquan Yi, Haiqiang Lin, Youzhu Yuan*

State Key Laboratory of Physical Chemistry of Solid Surfaces, National Engineering Laboratory for Green Chemical Productions of Alcohols-Ethers-Esters, College of Chemistry and Chemical Engineering, Xiamen University, Xiamen 361005, PR China

ARTICLE INFO

Article history:
Available online 28 October 2010

Keywords:
Ru
Carbon nanotubes
CO preferential oxidation
Confinement

ABSTRACT

5 wt.% Ru nanoparticles confined in the channels or dispersed on the outside surfaces of carbon nanotubes (CNTs) were prepared using ultrasonication-added capillarity action or deposition, affording two kinds of catalysts labeled as 5 wt.% Ru/CNTs-in and 5 wt.% Ru/CNTs-out. Characteristic studies by high-resolution transmission electron microscopy, X-ray powder diffraction and H_2-temperature programmed reduction revealed that the Ru nanoparticles existed in highly dispersion with a mean Ru particle size of 1.8 nm in the samples of 5 wt.% Ru/CNTs-in and 5 wt.% Ru/CNTs-out. The catalysts were evaluated for preferential oxidation of CO in hydrogen (CO-PROX). For a hydrogen-rich feed gas containing 1.0% CO and 1.0% O_2, the 5 wt.% Ru/CNTs-in catalyst showed the best activity with complete CO oxidation at the temperature window of 333–393 K. The CO-PROX performance at 373 K was stable for more than 100 h. However, lower CO conversion and narrower temperature window were obtained over the 5 wt.% Ru/CNTs-out catalyst and 5 wt.% Ru nanoparticles supported on other carriers under identical conditions. It is concluded that the nano-channels of CNTs can selectively increase the density of reactants and the encapsulation of Ru nanoparticles in the channels of CNTs can provide a micro-environment to reinforce the reactivity of catalytic sites.

1. Introduction

The polymer electrolyte membrane fuel cell (PEMFC) has been regarded as one of the most promising candidates for utilizing hydrogen to produce heat and electricity, especially for electric vehicles or residential co-generation systems [1]. However, Pt and Pt-based alloys, which are generally used as the anode of PEMFCs, are known to be easily poisoned by even small amounts of CO in the hydrogen-rich stream that can be produced from various hydrocarbons by the reforming and water gas shift (WGS) reactions [2], the remaining CO should be removed before reaching the PEMFC. Among the approaches investigated to remove the trace amount of CO in hydrogen-rich stream [3,4], the CO preferential oxidation (CO-PROX) has been considered to be suitable for sufficient CO removal.

To date, various supported noble metal catalysts, such as Pt, Ru, Au, Pd, and Rh, have been reported for the CO-PROX reaction in a hydrogen-rich gas [4–9]. In particular, the catalysts formulated with Pt have been most extensively tested [7,10–13]. However, they usually perform noticeable activities only under practical conditions above 423 K, at which temperature reverse WGS reactions can occur, thereby hindering complete CO removal. The Ru-based catalysts, like Ru/Al_2O_3, in some cases are reported to be more efficient for oxidizing CO than the other catalysts based on Pt, Pd, Rh, and Co under normal pressure conditions [7,14]. Nevertheless, there are still many efforts to enhance the CO-PROX activities of supported catalysts at low temperatures [9,15–17].

Carbon nanotubes (CNTs) with unique properties can play an important role in a large number of catalytic reactions [18]. Theoretical studies reveal that deviation of the graphene layers from planarity causes p-electron density to shift from the concave inner surface to the convex outer surface, leading to an electron deficient interior surface and an electron-enriched exterior surface [19]. In addition, studies on non-catalytic gas-phase reactions suggest that confinement within small channels could increase the density of reactants [20]. All of the characters can affect the catalytic activity for some reactions. Several studies have been reported on different positions of the catalyst center which supported on the CNTs, focusing on ethanol production [21], Fischer–Tropsch synthesis [22,23] and benzene hydrogenation [24]. Previously, we found that the CNTs-supported Pt catalysts (Pt/CNTs), in particular, the Pt/CNTs doped with Ni-MgO, were extremely active in the PROX reaction of CO [6,25]. However, the research on the enhancements of selective CO oxidation reaction over the CNTs-confined metal catalyst is scarce.

* Corresponding author. Tel.: +86 592 2181659; fax: +86 592 2183047.
E-mail address: yzyuan@xmu.edu.cn (Y. Yuan).

0920-5861/$ – see front matter © 2010 Elsevier B.V. All rights reserved.
doi:10.1016/j.cattod.2010.10.020

In this work, we have filled Ru nanoparticles into the inner surface of CNTs using ultrasonication-aided capillarity action. The CO-PROX reaction was performed to explore the confinement effect.

2. Experiments

2.1. Catalyst preparation

Multi-walled CNTs with outer diameter of 10–20 nm and the inner diameter of 4–8 nm were purchased from China Shenzhen Nano-port Co., Ltd. Al_2O_3, SiO_2, and graphite (GA) were purchased from Sinopharm Chemical Reagent Co., Ltd. Active carbon (AC) was purchased from Guangxi Yebao Active Carbon Co., Ltd and TiO_2 (P-25) was obtained from Degussa AG Co., Ltd. Prior to its use, the AC was pretreated in concentrated HNO_3 (68 wt.%) at 363 K for 4 h under reflux conditions to remove amorphous carbon. Meanwhile, Al_2O_3 was calcined in air at 873 K for 4 h.

The catalysts were prepared by referring to the procedure described in the literature with some modifications [21–24,26]. In order to fill the Ru species into the channel of CNTs, the as-received raw CNTs were treated with concentrated HNO_3 (68 wt.%) at 413 K for 14 h. The pretreated CNTs were then collected through filtration, washed several times with distilled water, and dried overnight under a vacuum at 353 K. Analysis by inductively coupled plasma optical emission spectrometer (ICP-OES) using a Thermo Electron IRIS Intrepid II XSP showed that the remaining Ni impurity in the CNTs was less than 0.002 wt.%. The acetone solution of $RuCl_3$ was introduced into the channels of CNTs utilizing the capillary forces aided by ultrasonication and stirring. The suspension was stirred for 12 h and evaporated at 333 K to remove the solvent. The solid obtained was dried under a vacuum at 353 K for 12 h. Before the catalytic reaction, the as-dried sample was activated by reduction in a flow of 5%H_2–95%N_2 at 673 K for 4 h. The final powder was labeled as Ru/CNTs-in catalyst. For the Ru/CNTs-out catalyst, the pretreated CNTs were impregnated in acetone with ultrasonication for 4 h. Then the acetone solution of $RuCl_3$ was added into the above suspension. After stirring for 1 h, the acetone was evaporated and the remained solids were subject to the same treatments of drying, heat-treatment, and reduction.

For comparison, the as-received raw CNTs were also treated with 6.0 mol l^{-1} aqueous HNO_3 solution at 363 K for 12 h. The treatment could remove amorphous carbon and most of Ni contamination but keep the caps closed. The remaining Ni impurity in the CNTs was less than 0.006 wt.% by ICP-OES. The product was denoted as CNTs-c. The catalysts of Ru/CNTs-c, Ru/GA, Ru/AC, Ru/SiO_2, Ru/Al_2O_3 and Ru/TiO_2 were prepared by the procedure similar to Ru/CNTs-out.

The nominal Ru loading was controlled to be 5 wt.%. The actual Ru content was determined by ICP-OES. The received values were 4.95 wt.% for Ru/CNTs-in, 4.93 wt.% for Ru/CNTs-out and 4.98 wt.% for Ru/CNTs-c.

2.2. Catalytic testing

The catalytic performance was examined in a conventional fixed-bed flow reactor using 100 mg of catalyst at 0.1 MPa as previously reported [27,28]. The reactant mixture was adjusted by mass flow controllers with compositions of $CO/O_2/H_2/N_2 = 1/1/50/48$ (mol.%) for PROX reaction and $CO/O_2/N_2 = 1/1/98$ for CO oxidation reaction. The ratio of total gaseous reactant flow rate to catalyst weight (F/W) was 30,000 ml h^{-1} g^{-1}. A steady conversion was attained after the reaction for 30 min at each temperature. The effluent gas was analyzed by an on-line gas chromatograph equipped with two packed columns (Molecular sieve 5A and Porapak Q) and thermal conductivity detector. The CO conversion and O_2 selectivity were calculated by the equations as reported elsewhere [27].

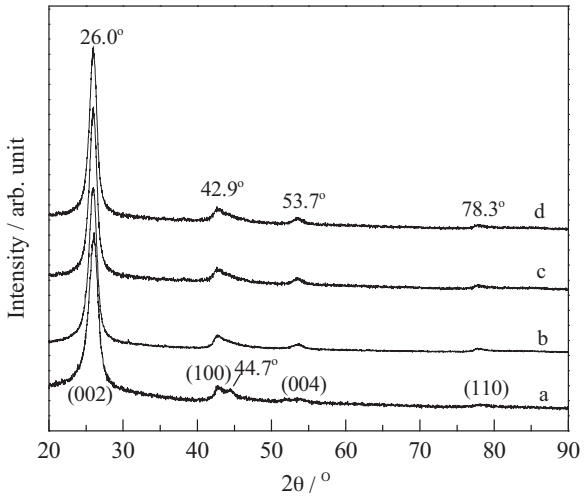

Fig. 1. XRD patterns of CNTs and 5 wt.% Ru/CNTs catalysts: (a) raw CNTs; (b) CNTs pretreated by 68% HNO_3 for 14 h at 140 °C; (c) 5 wt.% Ru/CNTs-in catalyst; (d) 5 wt.% Ru/CNTs-out catalyst.

2.3. High-resolution transmission electron microscopy and scanning electron microscope

Transmission electron microscopy (TEM) images were obtained on a Tecnai F30 electron microscope operated at an acceleration voltage of 300 kV. Samples for TEM measurements were ultrasonically dispersed in ethanol. Drops of suspensions were deposited on a copper grid coated with carbon. Scanning electron microscopy (SEM) images of the samples were obtained on a LEO 1530 scanning microscope operated at 10 eV. Prior to analysis, all the samples were gold coated in a sputter coating unit.

2.4. X-ray diffraction

X-ray diffraction (XRD) pattern was performed using a PANAlytical X'pert Pro. diffractometer equipped with a graphite monochrometer and Cu K_α radiation. The operation voltage and current were 40 kV and 30 mA, respectively.

2.5. H_2-temperature-programmed reduction

H_2-temperature-programmed reduction (H_2-TPR) profiles were measured in a fix bed continuous flow reactor connected to a Hiden Qic-20 mass spectrometer. In a typical measurement, the as-dried sample (50 mg) was reduced in a mixture of 5% H_2–95% Ar at a flow rate of 30 ml min^{-1} and heating rate of 10 K min^{-1}. The amount of H_2 consumption was measured using the mass spectrometer.

3. Results and discussion

The XRD patterns of CNTs and the supported Ru catalysts are shown in Fig. 1. Diffraction lines due to the raw CNTs were observed at $2\theta = 26.0°$, 42.9°, 44.7°, 53.7° and 78.3°. After pretreatment, the peak at $2\theta = 44.7°$ disappeared, indicating that almost residual Ni-catalyst for the production of CNTs was eliminated. The XRD patterns did not show any differences between the CNTs-supported Ru catalysts of 5 wt.% Ru/CNTs-in and 5 wt.% Ru/CNTs-out and the purified CNTs. The results implied that the size of metallic Ru crystallites was below 4 nm detectable limitation of XRD.

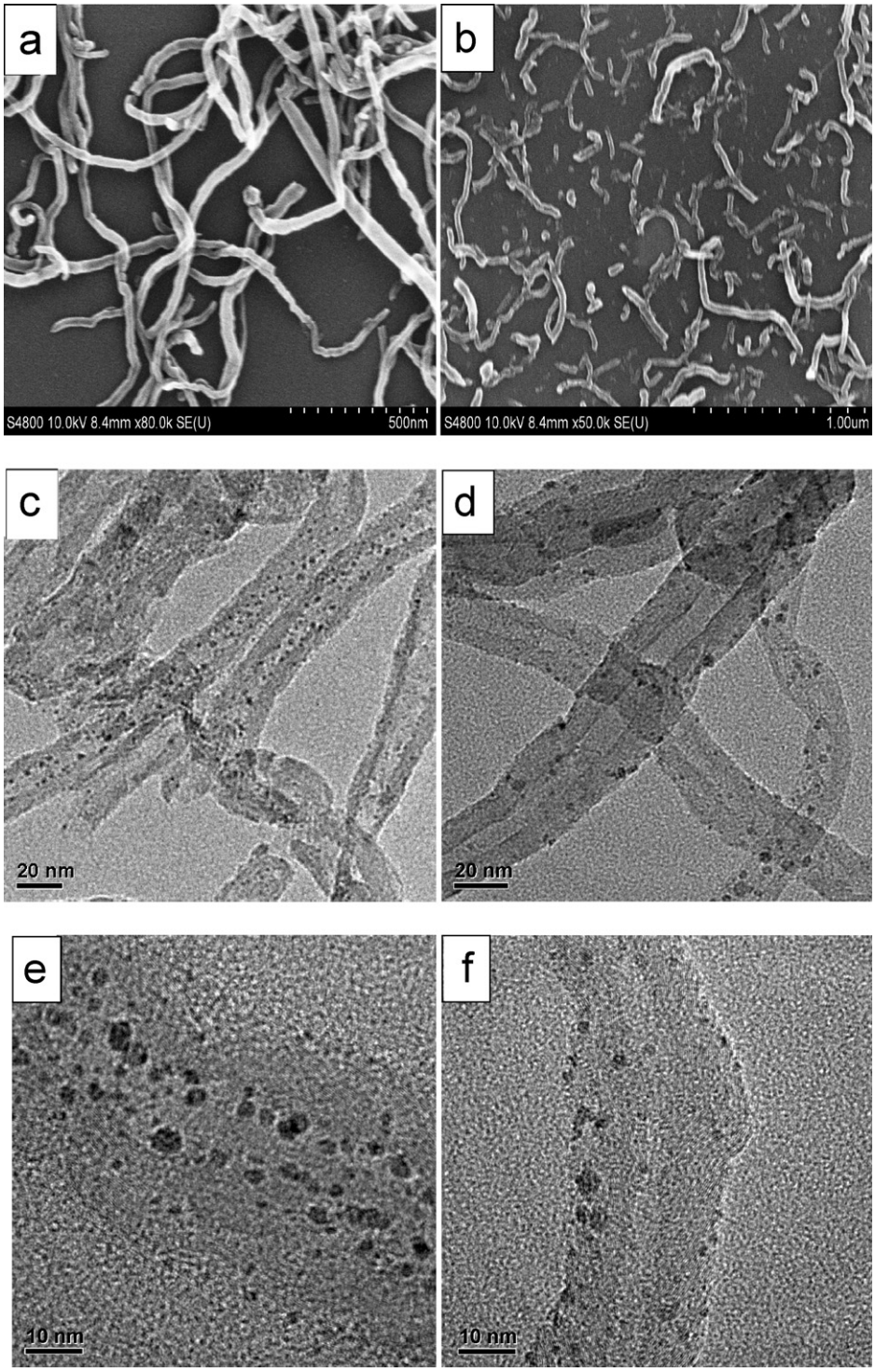

Fig. 2. SEM, TEM and HRTEM images of CNTs and 5 wt.% Ru/CNTs catalysts: (a) SEM image of raw CNTs; (b) SEM image of CNTs pretreated by 68% HNO_3 for 14 h at 140 °C; (c) TEM image of 5 wt.% Ru/CNTs-in catalyst; (d) TEM image of 5 wt.% Ru/CNTs-out catalyst; (e) HRTEM image of 5 wt.% Ru/CNTs-in catalyst; (f) HRTEM image of 5 wt.% Ru/CNTs-out catalyst.

The SEM image of raw CNTs in Fig. 2a shows that the sample contains solely CNTs without carbonaceous impurities and the woven nanotubes with high aspect ratios has length of 1–2 μm. After pretreatment with concentrated HNO_3 for 14 h, the raw CNTs were cut into shorter pieces with length of 100–500 nm and opened tips (Fig. 2b). The locations of Ru nanoparticles were verified using several TEM images (Fig. 2c–f). Fig. 2c shows that the Ru particles in the 5 wt.% Ru/CNTs-in are very uniform and most of them are located in the channels of CNTs with particle diameters around 1–2 nm. Fig. 2d shows that most of Ru particles in the 5 wt.% Ru/CNTs-out are well distributed on the outer surfaces of CNTs and their sizes are also rather uniforms (1–2 nm). The mean particle size in the 5 wt.% Ru/CNTs-in was estimated to be 1.8 nm, which was almost the same as that in the 5 wt.%Ru/CNTs-out. From the HRTEM images of two catalysts (Fig. 2e and f), we could clearly observe that the Ru nanoparticles were arranged along the inner wall of CNTs in the Ru/CNTs-in catalyst, while those were irregularly deposited on the outer surfaces of CNTs in the Ru/CNTs-out. Clearly, the size of Ru

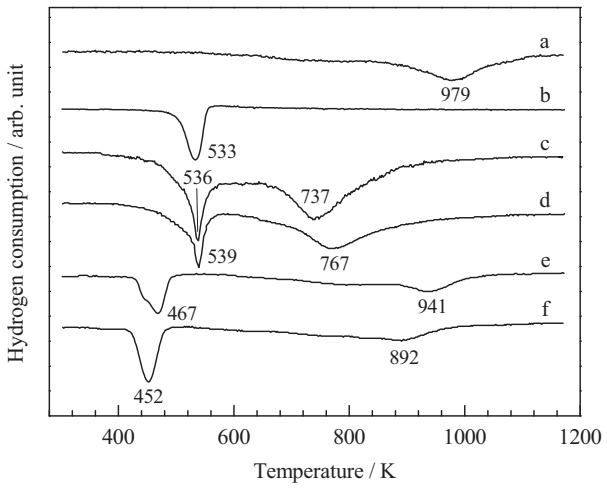

Fig. 3. H_2-TPR profiles of CNTs and Ru base catalysts: (a) CNTs pretreated by 68% HNO_3 for 14 h at 413 K; (b) $RuCl_3{\cdot}3H_2O$; (c) as-dried 5 wt.% Ru/CNTs-in; (d) as-dried 5 wt.% Ru/CNTs-out; (e) as-calcined 5 wt.% Ru/CNTs-out; (f) as-calcined 5 wt.% Ru/CNTs-in.

nanoparticles in the Ru/CNTs-in catalyst left sufficient space for the reactants and products diffusing in and out of the channels of CNTs.

H_2-TPR profiles of the as-dried samples of 5 wt.% Ru/CNTs-in and 5 wt.% Ru/CNTs-out are shown in Fig. 3. There were mainly two H_2 consumption peaks at the temperature range of 373–1173 K for the two samples. The first peak might be assigned to the reduction of Ru^{3+} species to metallic Ru, appearing at a temperature almost same to each other. The second peak that appeared at temperatures above 673 K was likely due to the reduction of carbon species on the surfaces of CNTs, since supported Ru nanoparticles could act as catalysts for the formation of methane *via* a reaction of hydrogen with the carbons on CNTs at higher temperatures. The phenomenon was also observed in previous studies on the CNTs-supported Fe and Fe–Ru catalysts [29,30]. However, the 5 wt.% Ru/CNTs-in sample gave lower reduction temperature for the second peak, which suggested that the Ru nanoparticles in the sample of 5 wt.% Ru/CNTs-in possessed a higher catalytic activity.

In previous reports [22–24], the metal oxides filled in the channels of CNTs always presented lower reduction temperatures in comparison to that supported on outside surfaces of CNTs. The decrease of reduction temperature of metal oxides which were filled in the channels of CNTs could be explained by the theory of electron-deficient interior surface of CNTs [31]. In the hollow concave surface of CNTs, the strengthened interaction between electron-deficient concave surface and anionic oxygen leads to weak the bonding strength of metal oxide bond, thereby the reducibility of metal oxides located inside the channels of CNTs is higher than that of ones in the outside surfaces of CNTs. We checked the H_2-TPR profiles of RuO_x deposited inside the channel and outside surfaces of CNTs. It was true that a lower reduction temperature for the RuO_x filled in the channels of CNTs could be observed as shown in Fig. 3f. Therefore, we deduced there might be different reduction behaviors between Ru^{3+} species and RuO_x. If the metallic Ru was directly reduced from Ru^{3+} species, there would be no significant differences in the reduction temperatures with respect to the Ru species located in the channels or on the outside surfaces of CNTs.

Table 1 compares the CO-PROX performances of Ru particles supported on several different carriers. It was manifested that CO was completely removed over the 5 wt.% Ru/CNTs-in catalyst with O_2 selectivity of 50% at the temperatures ranging from 333 to 393 K. However, the Ru/CNTs-out catalyst gave a CO conversion of 39.5% at 333 K and the highest CO conversion of 94.9% at 353 K. Similar result was also obtained on the Ru/CNTs-c catalyst, which afforded a CO conversion of 23.1% at 333 K and the highest CO conversion of 90.9% at 353 K. When the Ru nanoparticles were supported on other carriers, they showed lower CO-PROX performances under identical conditions. The results indicated that the changes of Ru particles electronic properties and the confinement effect of CNTs were beneficial for the removal of CO in a hydrogen-rich stream.

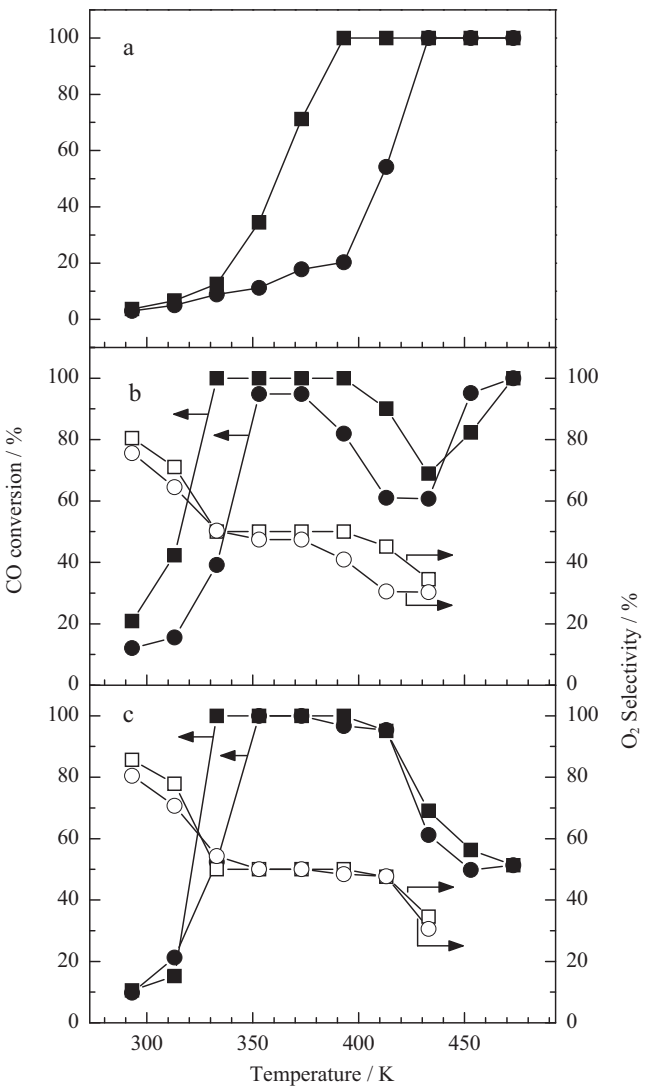

Fig. 4. The performances of CO oxidation and CO-PROX over 5 wt.% Ru/CNTs-in and 5 wt.% Ru/CNTs-out catalysts. (■) and (●): CO conversion over 5 wt.% Ru/CNTs-in and 5 wt.% Ru/CNTs-out, respectively; (□) and (○): O_2 selectivity over 5 wt.% Ru/CNTs-in and 5 wt.% Ru/CNTs-out, respectively. (a) CO oxidation on 5 wt.% Ru/CNTs-in and 5 wt.% Ru/CNTs-out. Reactants: 1.0% CO, 1.0% O_2, balanced with N_2; (b) CO-PROX performance on 5 wt.% Ru/CNTs-in and 5 wt.% Ru/CNTs-out. Reactants: 1.0% CO, 1.0% O_2, 50% H_2, balanced with N_2; (c) CO-PROX performance on 5 wt.% Ru/CNTs-in and 5 wt.% Ru/CNTs-out. Reactants: 1.0% CO, 1.0% O_2, 10% H_2, balanced with N_2.

Fig. 4 shows the results of CO oxidation and CO-PROX over the 5 wt.% Ru/CNTs-in and 5 wt.% Ru/CNTs-out catalysts as a function of temperature. For CO oxidation reaction, CO could be completely converted to CO_2 at 393 K on the 5 wt.% Ru/CNTs-in catalyst, while the complete CO oxidation occurred at 433 on the 5 wt.% Ru/CNTs-out catalyst (Fig. 4a). As for the CO-PROX reaction, the CO conversion reached 100% at 333 K on the 5 wt.% Ru/CNTs-in catalyst and such a performance could be maintained from 333 to 393 K. By contrast, the maximum CO conversion was only about 94.9% over

Table 1
The comparison of PROX performance over supported Ru catalysts with different carriers.

Catalyst (Ru loading = 5 wt.%)	CO conv./%		O_2 selec./%		The lowest temp. (K) for maximum CO conv.[a]
	At 333 K	At 393 K	At 333 K	At 393 K	
Ru/CNTs-c	23.1	80.4	70.2	40.2	353 (90.9)
Ru/CNTs-out	39.5	83.9	75.6	41.9	353 (94.9)
Ru/CNTs-in	100	100	50	50	333 (100)
Ru/AC[b]	15.2	80.6	60.7	40.3	353 (95.0)
Ru/GA[c]	9.1	76.8	67.2	38.4	473 (85.0)
Ru/Al_2O_3	28.2	95.2	81.3	47.6	373 (98.5)
Ru/TiO_2	12.3	51.7	34.9	25.9	433 (100)
Ru/SiO_2	20.8	54.5	56.2	27.3	373 (95.8)

Reaction conditions: Catalyst weight = 0.1 g, feed gas = CO (1.0%) + O_2 (1.0%) + H_2 (50%) + N_2 (48%), F/W = 30,000 ml h^{-1} g_{cat}^{-1}, reduction temperature of catalyst = 623 K.
[a] The data in parentheses are the CO conversion at this temperature.
[b] AC: active carbon.
[c] GA: graphite.

the 5 wt.% Ru/CNTs-out catalyst at 353 K (Fig. 4b). Nevertheless, at higher temperatures, the CO conversion decreased gradually both on the 5 wt.% Ru/CNTs-in and 5 wt.% Ru/CNTs-out catalysts due to the consumption of O_2 by H_2. The dropping rate for the CO conversion, however, was slower on the 5 wt.% Ru/CNTs-in catalyst. The above results again indicated that the deposition of catalytic active species on the inside channels of CNTs could enhance the catalyst activity.

In the CO-PROX reaction, the H_2 concentration was several times higher than CO. When the reactant gas was confined into the channels, the increase of CO density might be much more obvious than H_2, and thus the CO/H_2 ratio would be changed in the channel of CNTs. The effect might be one of the most important reasons for the enhanced performance. To gain insight into the increase of the density of reactants due to the confinement effect [32], we varied the H_2 concentration in the feed gas. The representative results are displayed in Fig. 4c. When the concentration of H_2 was significantly lowered down from 50% to 10%, the 5 wt.% Ru/CNTs-in catalyst could still perform a CO conversion of 100% at a wider temperature range of 333–393 K, while the 5 wt.% Ru/CNTs-out one could only exhibit a CO conversion of 100% at a narrower temperature range of 353–373 K. In this case, the O_2 selectivity for CO_2 formation over the two catalysts was almost same. Taking the results obtained at different H_2 concentrations into account, it was suggested that the ratios of CO/H_2 and O_2/H_2 in the channels of CNTs would be much higher than those in the outside surfaces of CNTs, even if in the case of dilute CO and O_2 in a hydrogen-rich stream, in virtue of the nano-channel confinement effect for enrichment of reactants [21–24]. The enrichment of CO and O_2 in the channels of CNTs increased the probability of CO reacted with O_2 and enhanced the O_2 selectivity. As a result, the CO conversion maintained 100% from 333 to 393 K on the Ru/CNTs-in catalyst in the case of H_2 concentration at either 10% or 50%. By contrast, the maximal CO conversion was lower than 100% on the Ru/CNTs-out catalyst in the case of H_2 concentration at 50%, which was essentially due to its lower selectivity of O_2 by the reaction of H_2 and O_2.

By comparing the performances of 5 wt.% Ru/CNTs-in and 5 wt.% Ru/CNTs-out catalysts at temperatures higher than 393 K, we found that the trends of CO conversion and O_2 selectivity on these two catalysts were almost the same to each other. The CO conversion increased in the 50% H_2 mixture (Fig. 4b) and decreased in the 10% H_2 mixture (Fig. 4c) on the either Ru/CNTs-in or Ru/CNTs-out catalysts at temperatures exceeding 430 K. This was essentially owing to the complete consumption of O_2 and the methanation of CO by H_2 at higher temperatures. Nonetheless, the methanation was less significant in the 10% H_2 mixture feed gas, resulting in a decrease of CO conversion at temperature above 430 K. The results indicated that higher H_2 concentration was beneficial for the CO methanation over the catalysts.

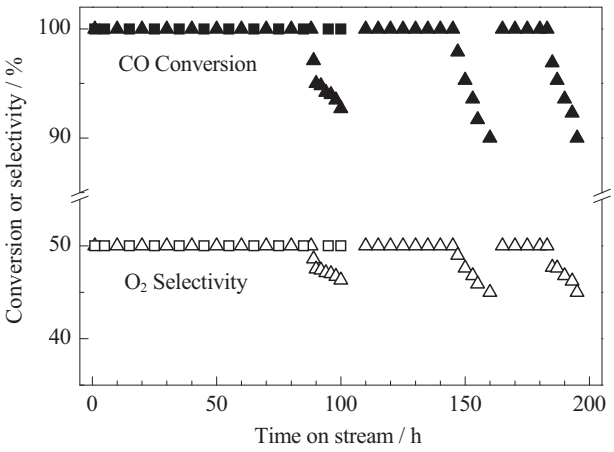

Fig. 5. CO-PROX over 5 wt.% Ru/CNTs-in catalyst as a function of reaction time at 373 K. (■) and (□): CO conversion and O_2 selectivity. Reactants: 1.0% CO, 1.0% O_2, 50% H_2, balanced with N_2; (▲) and (△): CO conversion and O_2 selectivity. Reactants: 1.0% CO, 1.0% O_2, 50% H_2, 19% CO_2, 10% H_2O, balanced with N_2.

The stability of CO-PROX reaction over the 5 wt.% Ru/CNTs-in catalyst is presented in Fig. 5. The catalyst could sustain 100% CO conversion and 50% O_2 selectivity for longer than 100 h at 373 K. Further prolonging the reaction time could cause a gradual drop in the CO conversion although which was still above 90%. When the CO-PROX reaction was conducted using a feed gas containing 19% CO_2 and 10% water vapor, 100% CO conversion and 50% selectivity of O_2 could be sustained for more than 85 h at 373 K. Moreover, the deactivated catalyst could be reused several times when the deactivated catalyst was reduced in a flow of 10%H_2–90%N_2 at 573 K for 4 h.

4. Conclusion

We have prepared a 5 wt.% Ru/CNTs-in catalyst with most of Ru nanoparticles confined in the channel of CNTs by a wet chemistry approach using ultrasonication-aided capillary action. The mean size of Ru particles in the channels of CNTs was around 1.8 nm. The results showed that the confinement of Ru nanoparticles in the channels of CNTs improved the catalytic performance for CO-PROX reaction, as being reflected by the wider operating temperature window of 333–393 K and good stability as long as 100 h at 373 K. The catalyst could also tolerate the existence of H_2O vapor and CO_2 in the feed gas and reuse several times. The enhanced performance was attributed to the micro-environment which reinforced the reactivity of catalytic sites and increased the density of reactants due to the nano-channels.

Acknowledgements

We acknowledge the financial supports from the National Natural Science Foundation of China (Nos. 20873108 and 20923004), the National Basic Research Program of China (No. 2009CB939804), and the Key Scientific Project of Fujian Province (No. 2009HZ0002-1).

References

[1] G. Hoogers, D. Thompsett, CATTECH 3 (1999) 106.
[2] L. Shore, R.J. Farrauto, in: W. Vielstich, A. Lamm, H.A. Gasteiger (Eds.), Handbook of Fuel Cells: Fundamentals, Technology and Applications, Part 2, vol. 3, Wiley, Chichester, 2003, pp. 211–218.
[3] D.L. Trimm, Appl. Catal. A: Gen. 296 (2005) 1.
[4] E.D. Park, D. Lee, H.C. Lee, Catal. Today 139 (2009) 280.
[5] S. Carrettin, P. Concepcion, A. Corma, J.M.L. Nieto, V.F. Puntes, Angew. Chem. Int. Ed. 43 (2004) 2538.
[6] K. Tanaka, M. Shou, H.B. Zhang, Y.Z. Yuan, T. Hagiwara, A. Fukuoka, J. Nakamura, D.L. Lu, Catal. Lett. 126 (2008) 89.
[7] P.V. Snytnikov, V.A. Sobyanin, V.D. Belyaev, P.G. Tsyrulnikov, N.B. Shitova, D.A. Shlyapin, Appl. Catal. A: Gen. 239 (2003) 149.
[8] Y.Q. Huang, A.Q. Wang, L. Li, X.D. Wang, D.S. Su, T. Zhang, J. Catal. 255 (2008) 144.
[9] Q. Fu, W.X. Li, Y.X. Yao, H.Y. Liu, H.Y. Su, D. Ma, X.K. Gu, L.M. Chen, Z. Wang, H. Zhang, B. Wang, X.H. Bao, Science 328 (2010) 1141.
[10] R. Padilla, M. Benito, L. Rodríguez, A. Serrano-Lotina, L. Daza, J. Power Sources 192 (2009) 114.
[11] A. Wootsch, C. Descorme, D. Duprez, J. Catal. 249 (2007) 318.
[12] O. Pozdnyakova, D. Teschner, A. Wootsch, J. Kröhnert, B. Steinhauer, H. Sauer, L. Toth, F.C. Jentoft, A. Knop-Gericke, Z. Paál, R. Schlögl, J. Catal. 237 (2006) 1.
[13] D. Teschner, A. Wootsch, O. Pozdnyakova-Tellinger, J. Kröhnert, E.M. Vass, M. Hävecker, S. Zafeiratos, P. Schnörch, P.C. Jentoft, A. Knop-Gericke, R. Schlögl, J. Catal. 249 (2007) 318.
[14] S. Oh, R.M. Sinkevitch, Catal. Rev. 43 (2001) 56.
[15] S.Y. Chin, O.S. Alexeev, M.D. Amiridis, J. Catal. 243 (2006) 329.
[16] T. Komatsu, A. Tamura, J. Catal. 258 (2008) 306.
[17] Y. Ishida, T. Ebashi, S. Ito, T. Kubota, K. Kunimoria, K. Tomishige, Chem. Commun. (2009) 5308.
[18] H.B. Zhang, G.D. Lin, Y.Z. Yuan, Cur. Top. Catal. 4 (2005) 1.
[19] M. Menon, A.N. Andriotis, G.E. Froudakis, Phys. Lett. 320 (2000) 425.
[20] E.E. Santiso, A.M. George, C.H. Turner, M.K. Kostov, K.E. Gubbins, B.N. Marco, S.B. Małgorzata, Appl. Surf. Sci. 252 (2005) 766.
[21] X.L. Pan, Z.L. Fan, W. Chen, Y.J. Ding, H.Y. Luo, X.H. Bao, Nat. Mater. 6 (2007) 507.
[22] M. Reza, M. Abbaslou, A. Tavassoli, J. Soltan, A.K. Dalai, Appl. Catal. A: Gen. 367 (2009) 47.
[23] W. Chen, Z.L. Fan, X.L. Pan, X.H. Bao, J. Am. Chem. Soc. 130 (2008) 9414.
[24] H.X. Yang, S.Q. Song, R.C. Rao, X.Z. Wang, Q. Yu, A.M. Zhang, J. Mol. Catal. A: Chem. 323 (2010) 33.
[25] H.W. Yang, G.Q. Yi, H.Q. Lin, K. Tanaka, Y.Z. Yuan, Chin. J. Catal. 30 (2009) 780.
[26] J.-P. Tessonnier, O. Ersen, G. Weinberg, C. Pham-Huu, D.S. Su, R. Schlög, ACS Nano 3 (2009) 2081.
[27] G.Q. Yi, Z.N. Xu, G.C. Guo, K. Tanaka, Y.Z. Yuan, Chem. Phys. Lett. 479 (2009) 128.
[28] G.Q. Yi, H.W. Yang, B.D. Li, H.Q. Lin, K. Tanaka, Y.Z. Yuan, Catal. Today (2010), doi:10.1016/j.cattod.2010.01.049.
[29] M.C. Bahome, L.L. Jewell, D. Hildebrandt, D. Glasser, N.J. Coville, Appl. Catal. A: Gen. 287 (2005) 60.
[30] M.C. Bahome, L.L. Jewell, K. Padayachy, D. Hildebrandt, D. Glasser, A.K. Datye, N.J. Coville, Appl. Catal. A: Gen. 328 (2007) 243.
[31] D. Ugarte, A. Chatelain, W.A. de Heer, Science 274 (1996) 1897.
[32] X.L. Pan, X.H. Bao, Chem. Commun. (2008) 6271.